2017

Impact of Flow Direction on Local Flow Behavior in Biologically-Inspired Flow Passages

Derrick Dewayne Herrin
dh04609

Impact of Flow Direction on Local Flow Behavior in Biologically-Inspired Flow Passages

An Honors Thesis submitted in partial fulfillment of the requirements for
Honors in Mechanical Engineering

By
Derrick Herrin

Under the mentorship of Dr. David Calamas

ABSTRACT

A computational fluid dynamics model was utilized to study the effect of flow direction on local flow behavior in biologically-inspired microscale flow networks. Biologically-inspired flow networks have been found to offer numerous advantages when compared with parallel flow networks, particularly in thermal management applications. Flow behavior was examined for a range of bifurcation angles and laminar inlet Reynolds numbers. The computational model was validated with existing theoretical solutions and verified for grid independence. As the bifurcation angle increased, the pressure drop, and thus pumping power, across the biologically-inspired flow networks increased. In addition, as the inlet Reynolds number increased, so did the pressure drop. Local spikes in pressure, which impacted the total pressure drop, were observed immediately following bifurcations. The magnitude of these changes in pressure was found to be dependent on bifurcation angle.

Thesis Mentor: _____
Dr. David Calamas

Honors Director: _____
Dr. Steven Engel

November 2017

Department of Mechanical Engineering

University Honors Program

Georgia Southern University

Acknowledgements

I would like to thank my faculty adviser, Dr. David Calamas, for his patience and guidance with this thesis. The time Dr. Calamas dedicated to this project cannot be understated, because without his help, this thesis would not have been possible.

I am so thankful for my Lord Jesus Christ who brought me through to the end. He is Faithful! Additionally, I would like to thank my church family for their continual prayers and support.

I would also like to thank the University Honors Program and my mechanical engineering family here at Georgia Southern University for all the laughs, guidance, and knowledge they have provided me with these past four years.

Last, but certainly not least, I would like to thank my girlfriend, family, and friends for their continued support of my collegiate career.

Table of Contents

List of Figures

List of Tables

Nomenclature

The following nomenclature is used in this thesis:

A	area (m^2)
d	diameter
Eu	Euler number
H	channel height (m)
h	hydraulic
I	moment of inertia
k	branch level
L	length (m)
n	number of bifurcations
P	pressure (Pa)
p	polar
Re	Reynolds number
u	average velocity (m/s)
V	velocity (m/s)
w	channel width (m)
X	non-dimensional axial distance
x	Cartesian coordinate (m)
y	Cartesian coordinate (m)
β	diameter-scale ratio
λ	length-scale ratio
μ	dynamic viscosity (kg/m·s)
ν	kinematic viscosity (m^2/s)
ρ	density (kg/m^3)

1. Introduction

1.1 Background and Motivation

Nature is an endless source of inspiration that guides the designs utilized by scientists and engineers. This design concept is most commonly known as biomimicry. Biologically-inspired flow systems have widely been analyzed for their effective thermal and fluid transport processes. Such phenomenon can easily be seen in mammalian circulatory and respiratory systems and also in the veins of tree leaves. Systems incorporating biologically-inspired flow passages produce space-filling flow networks, minimize flow resistance, and enhance surface area to volume ratios. Bifurcating, or fractal-like, flow networks have several advantages over traditional parallel flow networks. These advantages include lower pressure drop, increased surface temperature uniformity, and increased surface area per volume for heat transfer. Thus, biologically-inspired flow networks can be used in thermal management applications to increase thermal performance. What has not yet been studied is the impact of flow direction on local flow behavior in biologically-inspired microscale flow networks.

1.2 Objectives

The objective of the present work is to examine the impact of flow direction on local flow behavior in biologically-inspired flow networks. To accomplish this objective, a computational fluid dynamics model will be created. Upon validating the model's physics and ensuring a grid independent solution, the model will be used to study converging flow in biologically-inspired microscale flow networks for a range of bifurcation angles and inlet Reynolds numbers.

1.3 Literature Review

While there is research into micro channel fractal-like networks for turbulent and pulsatile flows available as well as for multiple phase convection medium, the current focus is on laminar, incompressible flow due to the mechanics of micro channel heat sinks. Research into this area started with work done on the blood circulatory system, a bifurcation network, where an optimization principle was discovered termed "Murray's Law" [1]. This law found that the optimal diameter of the blood vessel is proportional to the cube of the local velocity of the blood when the flow is laminar and numerous researchers experimentally validated this law as a general design principle for larger diameter networks. For smaller diameters, such as micro channels, a scaling factor of $2^{-1/2}$ was found to be true [2]. Investigation into further micro channel geometric optimization using constructal theory was started by Bejan et al. [3] and continued by many other researchers. Much research has been done on disk shaped micro channel tree like networks, parallel flow micro channel tree like networks, and micro channel fractal branching networks.

Pence et al. [4]compared fractal-like flow networks embedded in disk shaped heat sinks to parallel channel networks embedded in rectangular-shaped heat sinks by varying the number of branching levels, the number of parent branches, width of the terminal branch segment, channel depth and total channel length of the fractal-like network. Pence et al. found that for identical convective surface areas, the disk shaped tree like network has a lower wall temperature than a parallel micro channel network. Chen et al. [5] and Feng et al. [6] calculated a unit less critical radius that determines whether a radial or dendritic pattern of flow results in the lowest maximum temperature difference. Pence et

al. [7] compared a Y-shaped micro channel fractal branching network to a square parallel channel network with an identical plate surface area and found the tree like network had a 40% increase in thermal efficiency. Pence et al. also compared to a rectangular parallel channel network with an identical plate surface area and found the tree like network had a 45% decrease in thermal efficiency. Finally, Pence et al. concluded that increases in thermal efficiency for a fractal-like branching network is dependent on the foot print and channel spacing of a specific heat sink.

Wang et al. [8] compared a micro channel fractal branching network to a parallel micro channel network to find the impact of blockage on the wall temperatures for the tree like system. Wang et al discovered that the blockage in the upper level of the tree like network did not significantly affect wall temperature because of the complexity of the network. Wang et al concluded that increase of surface temperature uniformity and lower maximum wall temperatures could be accomplished by increasing the number of branch levels or increasing the number of branches coming from the inlet. Wechsatol et al. [9] examined a tree shaped micro channel network with loops. Wechsatol et al. concluded that loops could keep the flow from being blocked and although they cause an increase in flow resistance, as the network complexity increases, the flow resistance becomes relatively minor.

Hart et al. [10] varied the number of branch levels in their fractal like network and found that increasing complexity decreased pressure loss and increased the heat transfer rate. Hart et al. concluded that less pumping power and a more uniform wall temperature can be achieved by increasing the complexity of the fractal like network. Salimpour et al.

[11] investigated the optimal way to connect flow structures in a disk shaped body for minimization of both flow and thermal resistance while keeping one level of pairing. Salimpour, et al discovered that the thermal resistance decreases and the flow resistance increases as the level of network complexity increases. Chen et al. [12] [13] compared a fractal like network and a straight micro channel network analytically and experimentally to find that the fractal like branching micro channel had decreased pressure drop and increased heat transfer. Increase of the fractal dimension and number of branch levels caused an increase in heat transfer and decrease of pressure drop. Wechstaol et al. [14] investigated serpentine microchannel networks as compared to tree-shaped networks and found that the tree-shaped networks offered better global performance. Wechstaol et al. also discovered that the difference in performance between tree-shaped networks decreased as the level of complexity increased so very complex tree-shaped networks may not offer better performance than relatively simple tree-shaped networks. Wang et al. [15] compared the performance of serpentine microchannel networks and tree-like microchannel networks with 90° bifurcation angles to parallel microchannel network while keeping the convective surface area, channel volume and applied heat flux constant. Wang et al found that it is better to increase the number of distinct tree-like microchannel networks on a rectangular heat sink rather than to increase the number of branch levels for increased surface temperature uniformity. Additionally, Wang et al. found that serpentine microchannels have more uniform surface temperatures as compared to parallel microchannels but at the expense of higher pumping power requirements. Wang et al. [16] investigated the difference in pressure drop and maximum wall temperatures for a symmetric tree-like flow

network, a symmetric leaf-like flow network, and an asymmetric (offset) leaf-like flow network, all without loops. Wang et al. found that symmetric leaf-like flow network resulted in the lowest maximum wall temperatures and had a lower pressure drop as compared to the symmetric tree-like flow network.

Wang et al. [17] examined the effect of a range of uniform bifurcation angles on the surface uniformity and pressure drop of a diverging fractal-like network. Wang et al. found that there was local pressure recovery at the bifurcation and that the pressure drop in the system with every bifurcation angle was lower than the pressure drop in an equivalent parallel channel flow network. Wang et al. discovered that the pressure drop was less with smaller bifurcation angles. Finally, Wang et al. found the small bifurcation angles had surface temperature spikes in the higher order branches while the larger bifurcation angles had surface temperature spikes in the lower order branches.

Zhang et al. [18] investigated a fractal like branching network at different Reynolds numbers and aspect ratio and found secondary flow and recirculation at the 180 degree bifurcations and 90 degree bends. Zhang et al. determined that the secondary flow and recirculation were causing increased heat transfer due to mixing and an increased pressure drop. The vorticity of the flow increased as the Reynolds and the aspect ratio decreased. Yu et al. [19] investigated the relationship of the aspect ratio pressure drop and the average heat transfer coefficients for a micro scale fractal like network using a comparable straight parallel network. With the symmetric bifurcation at a constant angle of 180 degrees, three different aspect ratios were run for both networks. Yu et al. found that as the aspect ratio increased, the pressure drop increased. Yu et al. determined that the average heat transfer

coefficient increased with the aspect ratio at the cost of increased necessary pumping power.

Upon assessing the literature, it was apparent that flow behavior had only been examined in biologically-inspired flow networks with diverging flow passages. It is the objective of the present work to reverse the direction of flow and examine how the flow direction impacts local flow behavior. This will be done for a range of laminar inlet Reynolds numbers and bifurcation angles.

1.4 Description of Tree-Like Flow Networks

The nomenclature and coordinate system describing the tree-like flow networks utilized in the present analysis can be seen in Fig. 1. The first branch emanating from the inlet plenum is defined as the zeroth-order branch, where k = 0, and the last branch is defined as the third-order branch, where k = 3. The total length is defined as the radial distance between the entrance of the k = 0 branch and the exit of the k = 3 branch. The branch lengths are measured radially as seen in Fig. 1.

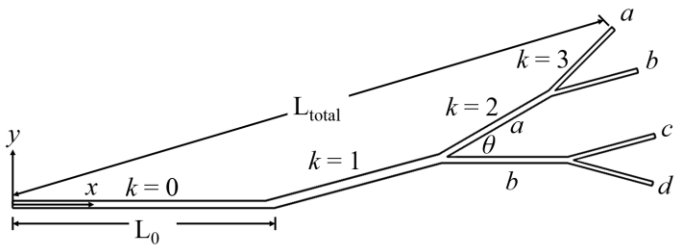

Figure 1 Nomenclature and Coordinate System

The flow network is symmetric and the bifurcation angles are independent of the path taken. In order to characterize the flow of the fluid through the tree-like network, two different paths are defined. Path 1 consists of the branch segments k = 0, 1, 2a, and 3a. Path

2 consists of the branch segments, k = 0, 1, 2b, and 3c. Paths 1 and 2 thus share the zeroth and first-order branch level. The bifurcation angle is defined as the angle from which a higher level branch splits from a lower level branch. Three different bifurcation angles were investigated: 15, 30, and 45°. In the design of the biologically-inspired flow networks, the following branch scale ratios were utilized:

$$\beta = \frac{d_{k+1}}{d_k} = n^{-\frac{1}{3}} \quad (1)$$

$$\gamma = \frac{L_{k+1}}{L_k} = n^{-\frac{1}{2}} \quad (2)$$

For this analysis, n = 2 as each parent channel splits into 2 daughter channels. A daughter branch thus has a length that is $2^{-1/2}$ times shorter and a hydraulic diameter $2^{-1/3}$ times smaller than its parent branch. The geometry and dimensions of the microscale biologically-inspired networks can be seen in Table 1.

Table 1 Dimensions of Microscale Flow Networks

k	H_k (mm)	w_k (mm)	d_k (mm)	L_k (mm)
0	0.500	1.000	0.667	7.12
1	0.500	0.794	0.613	5.02
2	0.500	0.630	0.557	3.56
3	0.500	0.500	0.500	2.52

2. Computational Methodology

2.1 Governing Equations

Numerical simulations were performed using the finite-volume based, commercially available, Computational Fluid Dynamics (CFD) software ANSYS Fluent (version 17.1). The working fluid was assumed to be water with constant thermophysical properties. The value for the thermophysical properties of the working fluid were evaluated at standard atmospheric temperature and pressure. The governing equations and simplifying assumptions are shown below. The equation for conservation of mass, or the continuity equation, can be written as follows

$$\frac{\partial \rho}{\partial t} + \nabla(\rho \vec{v}) = 0 \tag{3}$$

Assuming a steady state, the continuity equation can be reduced to

$$\nabla(\rho \vec{v}) = 0 \tag{4}$$

Assuming an incompressible flow, the continuity equation can be further reduced to

$$\nabla(\vec{v}) = 0 \tag{5}$$

The conservation of momentum can be written as

$$\frac{\partial}{\partial t}(\rho \vec{v}) + \nabla(\rho \vec{v}\vec{v}) = -\nabla p + \nabla(\bar{\bar{\tau}}) + \rho \vec{g} \tag{6}$$

Assuming a steady state again, the momentum equation can be reduced to

$$\nabla(\rho \vec{v}\vec{v}) = -\nabla p + \nabla(\bar{\bar{\tau}}) + \rho \vec{g} \tag{7}$$

If gravitational body forces can be neglected the momentum equation can be further reduced to

$$\nabla(\rho\vec{v}\vec{v}) = -\nabla p + \nabla(\bar{\bar{\tau}}) \tag{8}$$

where stress tensor is given by

$$\bar{\bar{\tau}} = \mu\nabla\vec{v} \tag{9}$$

Substituting the stress tensor in the momentum equation yields

$$\nabla \cdot (\rho\vec{v}\vec{v}) = -\nabla p + \nabla \cdot (\mu\nabla\vec{v}) \tag{10}$$

Assuming the density and viscosity are constant, the momentum equation can be written as

$$\rho(\nabla(\vec{v}\vec{v})) = -\nabla p + \mu\nabla^2(\vec{v}) \tag{11}$$

The boundary conditions can be seen in Fig. 2 below. A uniform velocity profile was assumed at the inlet. The magnitude of the velocity at the inlet corresponded to an inlet Reynolds number between 500 and 1750 based off of the hydraulic diameter at the inlet. It was assumed that there was no-slip at channel walls. All of the walls were assumed to be adiabatic as heat transfer was not considered in this analysis. The flow discharged via a pressure opening at atmospheric pressure.

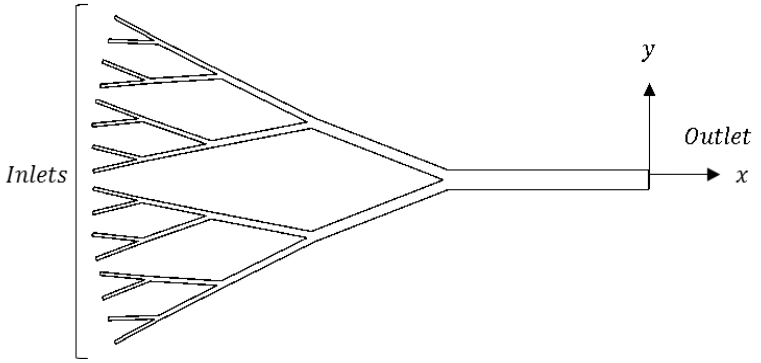

Figure 2 Converging Flow Coordinate System

2.2 Solution Methods

As previously mentioned, a steady-state was assumed. A pressure-based solver that uses a solution algorithm where the governing equations are solved sequentially was utilized. The flow was assumed to be laminar. Pressure-velocity coupling was achieved via the SIMPLE (Semi-Implicit Method for Pressure Linked Equations) method which uses a relationship between velocity and pressure corrections to enforce mass conversation and to obtain the pressure field.

The CFD software stores discrete values of field variables at cell centers. However, face values are required for the convective term and must be interpolated from the cell center values. This was accomplished via the QUICK (Quadratic Upstream Interpolation for Convective Kinematics) scheme due to the use of hexahedral elements. A second order scheme was utilized to interpolate pressure values at cell faces. Gradients required to construct scalar values of field variables at cell faces as well as for determining secondary diffusion terms and velocity derivatives were calculated according to the Least Squares Cell-Based method.

The pressure based solver utilizes under-relaxation to control the update of computed variables at each iteration. Under-relaxation factors for pressure and momentum were 0.3 and 0.7. As heat transfer was not considered, and thus temperature was not coupled with the momentum equations, the under-relaxation factor for temperature was set to 1.0.

2.3 Validation

In order to validate the physics of the computational model, a rectangular microchannel with a length ten times longer than the hydrodynamic entrance length was created. The pressure drop across the computational model was compared to the theoretical pressure drop predicted by Bahrami et al. [20] for fully developed laminar flow in a microchannel. In order to input a fully developed (non-uniform) velocity profile at the inlet, the velocity profile at the outlet of the channel, where the flow was fully-developed was recorded. This fully-developed outlet velocity profile was then inserted as the inlet velocity to ensure fully-developed flow throughout the channel. A uniform inlet velocity and fully-developed outlet velocity can be seen in Figure 3 below.

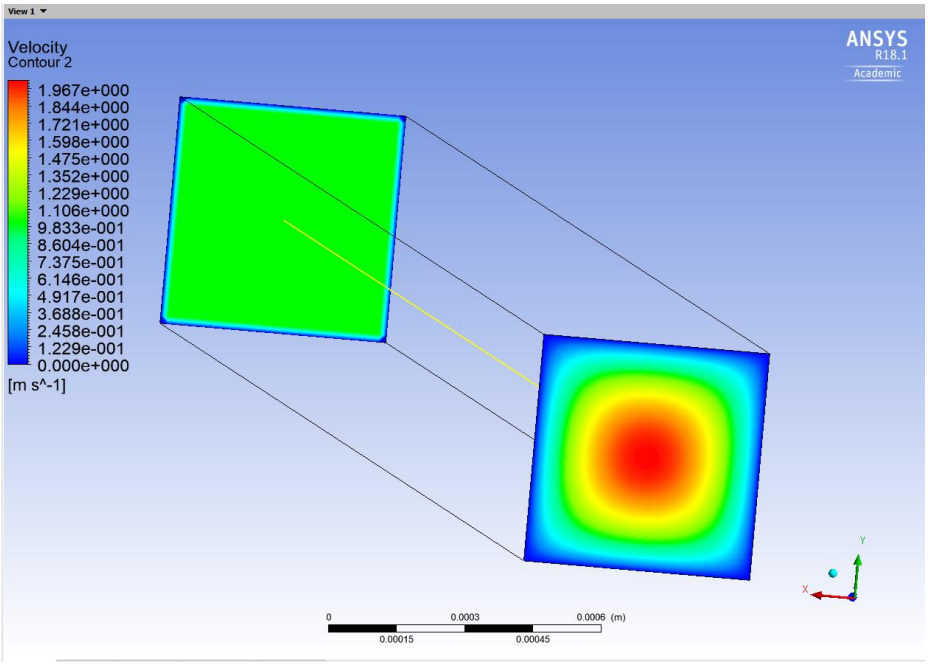

Figure 3 Uniform to Fully-Developed Velocity Profile

The theoretical value for the pressure drop as predicted by Baharmi [20] is only a function of geometrical parameters of the cross-section, i.e., area, perimeter and polar moment of inertia. The channel aspect ratio is defined as

$$\varepsilon = \frac{H}{w} \tag{12}$$

The polar moment of inertia for a rectangular cross-section is defined as

$$I_p = \frac{1 + \varepsilon^2}{12\varepsilon} \tag{13}$$

The pressure drop across the straight microchannel of rectangular cross-section for fully developed laminar flow is

$$\Delta P = \frac{16\pi^2 \mu u}{A} I_p L \tag{14}$$

As the theoretical equation used to predict the pressure drop in a straight, rectangular, microchannel was only valid for laminar flow, the computational model was validated for Reynolds numbers of 250, 500, 1000, 1500 and 1750. The difference between the theoretical and computational pressure drop across the straight, rectangular, microchannel can be seen in Fig. 4.

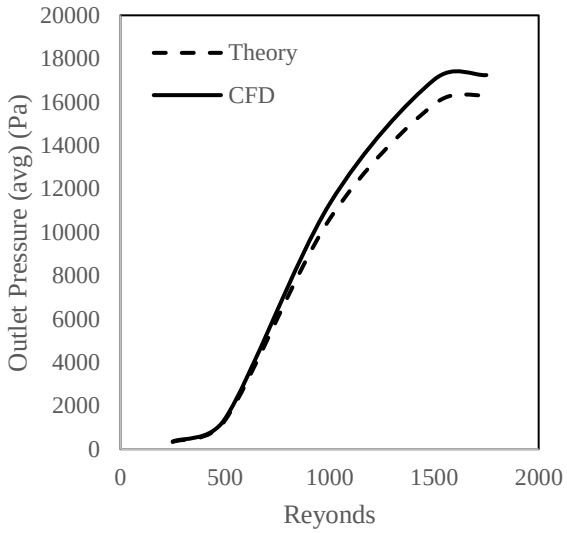

Figure 4 Computational Model Validation

2.4 Verification

In order to ensure a grid-independent solution, a mesh sensitivity analysis was performed. To verify a grid-independent solution the number of cells across the channels, in each direction, was increased until the solution no longer changed. This was done for each of the biologically-inspired flow networks. An example of the grid-independence procedure can be seen in the figure below for the biologically-inspired flow network with a bifurcation angle of 45°.

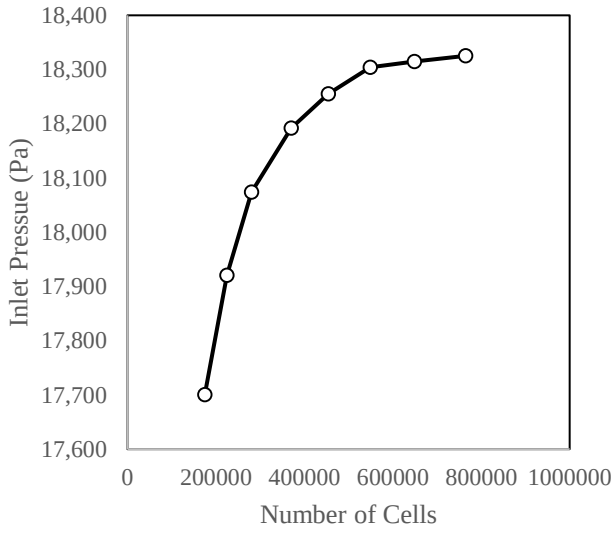

Figure 5 Computational Model Verification

3. Results and Discussion

3.1 Dimensionless Numbers

The performance of a microscale, flow network were analyzed for inlet Reynolds numbers of 500, 1000, and 1750. In addition, three different flow networks, with symmetric bifurcation angles of 15, 30, and 45° were investigated. The results were cast in dimensionless form for ease of scaling comparison. The dimensionless axial distance is defined as

$$X = \frac{x}{L_{total}} \tag{15}$$

where x is the distance along the centerline of the channel in the x direction and L_{total} is the total channel length as defined in Fig. 1. The Reynolds number is the ratio of inertia to viscous forces and is defined as

$$Re = \frac{VD_h}{\nu} \tag{16}$$

where V is the average velocity at the inlet, D_h is the hydraulic diameter at the inlet, and ν is the kinematic viscosity of water. The Euler number is the ratio of pressure to inertia forces and is defined as

$$Eu = \frac{\Delta P}{\rho V^2} \tag{17}$$

where ΔP is the relative pressure, V is the average fluid velocity and ρ is the density of the working fluid, water.

3.2 Velocity Contours

The flow behavior through the tree-like flow networks is dependent upon bifurcation angle. Velocity contours along the center plane of the biologically-inspired flow networks can be seen in the figures below. The flow accelerates, due to conservation of mass, after each of the bifurcations. In addition, as the bifurcation angle increases, so does the level of flow separation away from the wall.

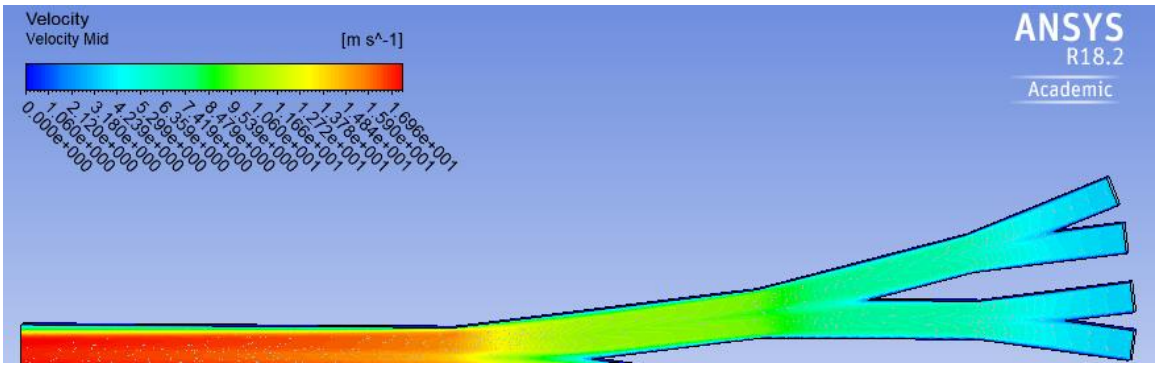

Figure 6 Mid-Depth Velocity Contours (Re = 1750, θ = 15°)

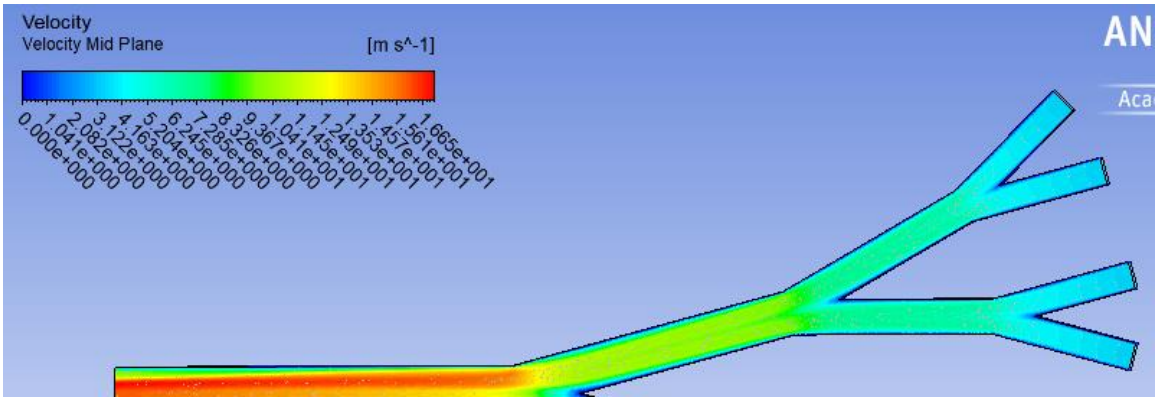

Figure 7 Mid-Depth Velocity Contours (Re = 1750, θ = 30°)

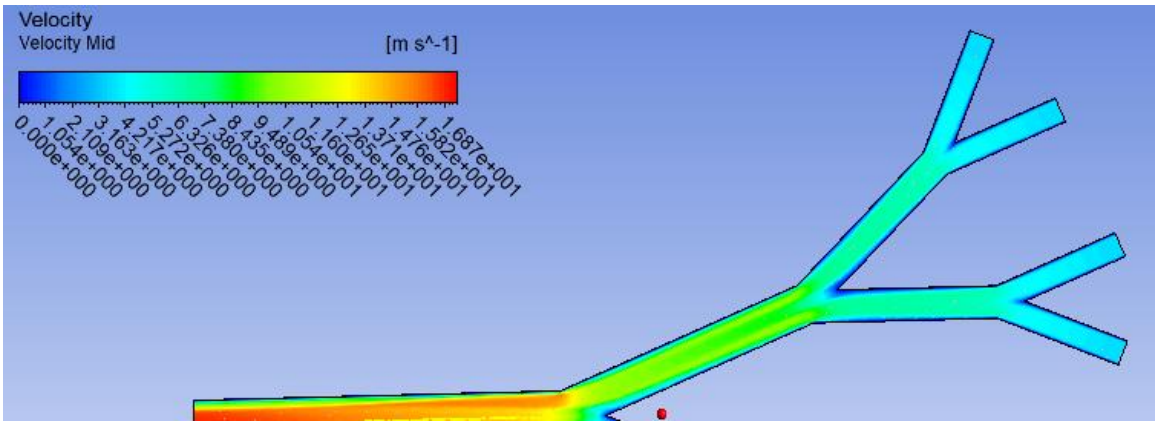

Figure 8 Mid-Depth Velocity Contours (Re = 1750, θ = 45°)

3.3 Local Flow Behavior at Bifurcations

The centerline Euler number distributions along paths 1 and 2 (see Section 1.4) can be seen in the figures below. As previously mentioned, the Euler number represents the ratio of pressure to inertia forces in the flow. An increase in the Euler number is associated with an increase in pressure. The local pressure is highly dependent upon bifurcation angle. Larger changes in pressure are present as the bifurcation angle is increased from 15 to 45°.

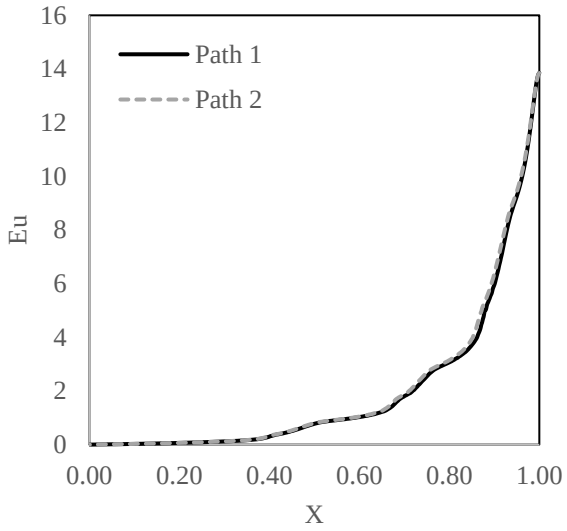

Figure 9 Path-Dependent Euler Number (Re = 1000, θ = 15°)

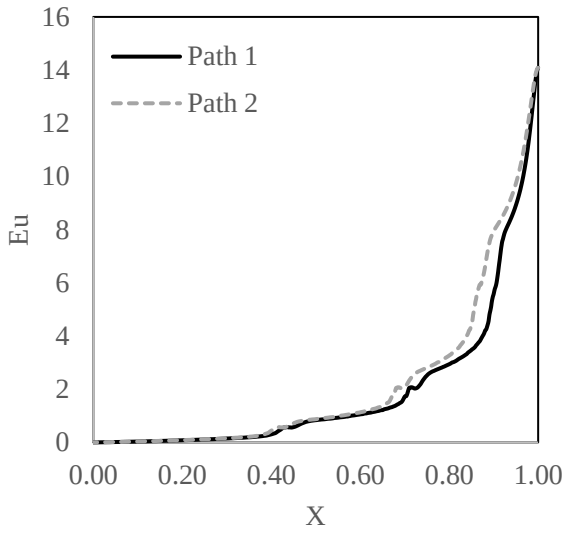

Figure 10 Path-Dependent Euler Number (Re = 1000, θ = 30°)

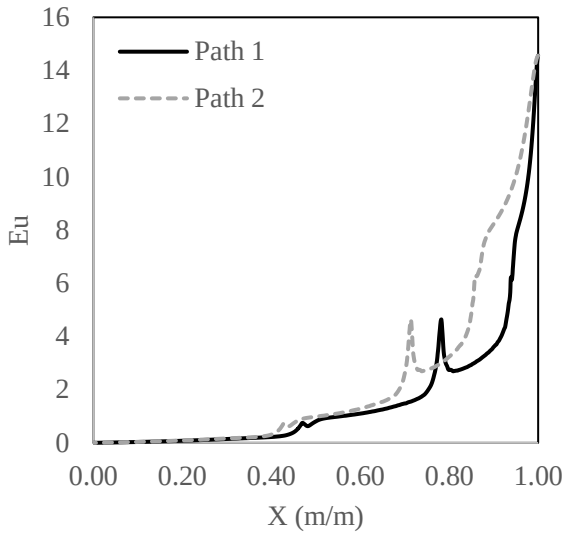

Figure 11 Path-Dependent Euler Number (Re = 1000, θ = 45°)

3.4 Further Discussion

The lowest total pressure drop was achieved when the bifurcation angle was the smallest. As the bifurcation angle is decreased, the fluid follows a less complex flow path and less flow separation is observed at bifurcations. In addition, the lower the bifurcation angle, the lower the total surface area of the flow network. Therefore, a flow network with a smaller surface area is expected to have a lower total pressure drop due to less friction with the channel walls. The magnitude of pressure spikes at bifurcation is highly dependent upon bifurcation angles with the largest spikes observed in the 45° flow network, regardless of inlet Reynolds number. Local changes in pressure were minimal in the 15° network. The highest increases in pressure were observed after the second bifurcation. This is in contrast to Wang et al. [17] who found the largest increases in pressure occurred after the first bifurcation. However, in this analysis the flow was converging while in Wang et al. analysis the flow was diverging. The flow direction thus clearly impacts local pressure

spikes at bifurcations. The pressure increases along path 2 were larger then that along path 1 due to the changes in the direction of the flow.

4. Conclusion

A computational fluid dynamics analysis was performed to assess the impact of flow direction on local flow behavior in biologically-inspired flow networks. The computational model was validated with a theoretical model on the basis of total pressure drop. In addition, the model was verified for grid-independence through a mesh-sensitivity analysis. The total pressure drop was found to increase as the bifurcation angle increased due to an increase in flow area as well as a more complex flow path. Local flow behavior was found to be dependent upon the path taken. The largest changes in pressure were observed following the second bifurcation, regardless of bifurcation angle and inlet Reynolds number. Finally, as the Reynolds number increased so did the pressure drop across the flow networks.

References

[1] C. D. Murray, "The Physiological Principle of Minimum Work: I. The Vascular System and the Cost of Blood Volume," *Proceedings of the National Academy of Sciences of the United States of America,* vol. 12, no. 3, pp. 207-214, 1926.

[2] P. Xu, B. Yu, M. Yun and M. Zou, "Heat Conduction in Fractal Tree-Like Branching Networks," *International Journal of Heat and Mass Transfer,* vol. 49, no. 19-20, pp. 3746-3751, 2006.

[3] A. Bejan, "Constructal-Theory Network of Conducting Paths for Cooling a Heat Generating VOlume," *International Journal of Heat and Mass Transfer,* vol. 40, no. 4, pp. 799-816, 1997.

[4] D. V. Pence, "Reduced Pumping Power and Wall Temperature in Microchannel Heat Sinks with Fractal-Like Branching Channel Networks," *Microscale Thermophysical Engineering,* vol. 6, no. 4, pp. 319-330, 2003.

[5] L. Chen, H. Feng, Z. Xie and F. Sun, "Constructal Optimization for "Disc-Point" Heat Conduction at Micro and Nanoscales," *International Journal of Heat and Mass Transfer,* vol. 67, pp. 704-711, 2013.

[6] H. Feng, L. Chen, Z. Xie and F. Sun, "Constructal Optimization of a Disc-Shaped Body with Cooling Channels for Specified Pumping," *International Journal of Low Carbon Technologies,* vol. 10, pp. 229-237, 2015.

[7] D. V. Pence, "Improved Thermal Efficiency and Temperature Uniformity Using Fractal-Like Branching Channel Networks," in *Heat Transfer & Transport Phenomena in Microscale*, G. P. Celata, Ed., New York, Begell House, 2000, pp. 142-148.

[8] X. Q. Wang, A. S. Mujumdar and C. Yap, "Numerical Analysis of Blockage and Optimization of Heat Transfer Performance of Fractal-Like Microchannel Nets," *Journal of Electronic Packaging,* vol. 128, no. 1, pp. 38-45, 2006.

[9] W. Wechsatol, S. Lorente and A. Bejan, "Tree-Shaped INsulated Designs for the Uniform Distribution of Hot Water Over an Area," *International Journal of Heat and Mass Transfer,* vol. 44, pp. 3111-3123, 2001.

[10] R. A. Hart and A. K. da Silva, "Experimental Thermla-Hydraulic Evaluation of Constructal Microfluidic Structures Under Fully Constrained Conditions," *International Journal of Heat and Mass Transfer,* vol. 54, pp. 3661-3671, 2011.

[11] M. R. Salimpour and A. Menbari, "Analytical Optimization of Constructal Channels Used for Cooling a Ring Shaped Body Based on Minimum Flow and Thermal Resistances," *Energy,* vol. 81, pp. 645-651, 2015.

[12] Y. Chen and P. Cheng, "Heat Transfer and Pressure Drop in Fractal Tree-Like Microchannel Nets," *International Journal of Heat and Mass Transfer,* vol. 45, pp. 2643-2648, 2002.

[13] Y. Chen and P. Cheng, "An Experimental INvestigation on the Thermal Efficiency of Fractal Tree-Like Microchannel Nets," *International Communications in Heat and Mass Transfer,* vol. 32, no. 7, pp. 931-938, 2005.

[14] W. Wechsatol, S. Lorente and A. Bejan, "Dentritic Heat Convection on a Disc," *International Journal of Heat and Mass Transfer,* vol. 46, pp. 4381-4391, 2003.

[15] X. Q. Wang, A. S. Mujumdar and C. Yap, "Thermal Characteristics of Tree-Shaped Microchannel Nets for Cooling of a Rectangular Heat Sink," *International Journal of Thermal Sciences,* vol. 45, no. 11, pp. 1103-1112, 2006.

[16] X. Q. Wang, A. S. Mujumdar and C. Yap, "Flow and Thermal Characteristics of Offset Branching Network," *International Journal of Thermal Sciences,* vol. 49, no. 2, pp. 272-280, 2010.

[17] X. Q. Wang, A. S. Mujumdar and C. Yap, "Effect of Bifurcation Angle in Tree-Shaped Microchannel Networks," *Journal of Applied Physics,* vol. 102, no. 7, 2007.

[18] C. Zhang, Y. Lian, C. Hsu, J. Teng, S. Liu, Y. Chang and R. Greif, "Investigations of Thermal and FLow Behaviour of Bifurcations and Bends in Fractal_like Microchannel Networks: Secondary Flow and Recirculation Flow," *International Journal of Heat and Mass Transfer,* vol. 85, pp. 723-731, 2015.

[19] X. F. Yu, C. P. Zhang, J. T. Teng, S. Y. Huang, S. P. Jin, Y. F. Lina, C. H. Cheng, T. T. Xu, J. C. Chu, Y. J. Chang, T. Dang and R. Greif, "A Study on the Hydraulic and Thermal Characteristics in Fractal Tree-Like Microchannels by Numerical and Experimental Methods," *International Journal of Heat and Mass Transfer,* vol. 55, pp. 7499-7507, 2012.

[20] M. Bahrami, M. M. Yovanovich and J. R. Culham, "Pressure Drop of Fully-Developed, Laminar Flow in Microchannels of Arbirtray Cross-Section," *Journal of Fluids Engineering*, vol. 128, pp. 1036-1044, 2006.